

Original paper

# The role of diffusion-weighted imaging in the evaluation of adnexal lesions

Annapura Srirambhatla<sup>1,A,B,C,D,E,F</sup>, Roopa Devi Hosamani<sup>2,A,B,C,D,F</sup>, Eshwar Chandra Nandury<sup>3,A,B,D</sup>

<sup>1</sup>All India Institute of Medical Sciences, Hyderabad, India

<sup>2</sup>Kamineni Hospitals, L.B. Nagar, Hyderabad, India

<sup>3</sup>Virinchi Hospitals, Hyderabad, India

## Abstract

**Purpose:** Magnetic resonance imaging (MRI) has been used as a problem-solving tool in the diagnosis of adnexal lesions. Both benign and malignant ovarian masses can present as complex adnexal lesions. Preoperative diagnosis of malignancy is essential for planning the surgical approach and appropriate treatment regimen. The aim of our study was to determine the role of diffusion-weighted MRI (DWI) in differentiating benign from malignant adnexal lesions.

**Material and methods:** Fifty-five patients (constituting 67 lesions) referred to MRI for evaluation of adnexal lesions were studied using 1.5 T MRI. The signal on DWI (qualitative) and ADC values (quantitative DWI) of the solid and cystic components of the lesions were analysed separately. Chi-square test, cross tabulation, and ROC curves were used to determine features on DWI that could distinguish benign from malignant lesions.

**Results:** Of the 67 lesions, 50 were benign and 17 were malignant. There was a significant association of hyperintense signal of solid components on T2W and DWI with malignancy, with a p-value of 0.003 and 0.001, respectively. Benign lesions showed hypointense signal on T2W and DWI. ADC values of the solid components could not distinguish benign from malignant lesions;  $p = 0.290$ . The signal intensity and ADC values of the cystic fluid in benign and malignant lesions showed a significant overlap.

**Conclusions:** Qualitative DWI acts as an adjunct to conventional MRI in differentiating benign from malignant adnexal lesions showing solid/mixed morphology. It plays no role in distinguishing lesions based on their cystic components. ADC values play no role in differentiating benign from malignant adnexal lesions irrespective of lesion morphology.

**Key words:** diffusion-weighted imaging, ADC value, ovarian malignancy, endometriotic cysts, adnexal lesions.

## Introduction

Increased use of ultrasound (USG) for diagnosing abdominal and gynaecological abnormalities has increased the detection of adnexal lesions (both symptomatic and otherwise). It is of utmost importance to determine if an adnexal lesion is benign or malignant because it has a significant bearing on its management and follow-up.

Transvaginal ultrasound is the primary imaging modality for evaluating adnexal pathology. Characterization of adnexal lesions is accurate when they show specific

features on ultrasound as per IOTA (International Ovarian Tumour Analysis Group) [1]. However, the characterization becomes difficult when the lesions are complex and large.

Owing to its better tissue characterization, spatial resolution, and multiparametric features, magnetic resonance imaging (MRI) has been used as a problem-solving tool in the diagnosis of complex adnexal lesions. Conventional MRI sequences help in tissue characterization and show a high specificity in the diagnosis of benign ovarian lesions. Diffusion-weighted imaging (DWI) has been used

## Correspondence address:

Annapura Srirambhatla, All India Institute of Medical Sciences, Hyderabad, India, phone: 091 9676888781, e-mail: [purnasrirambhat@gmail.com](mailto:purnasrirambhat@gmail.com)

## Authors' contribution:

A Study design · B Data collection · C Statistical analysis · D Data interpretation · E Manuscript preparation · F Literature search · G Funds collection

for the differentiation of benign from malignant lesions in gynaecological imaging [2,3].

The aim of our study was to determine the role of diffusion-weighted MRI in differentiating benign from malignant adnexal lesions, to describe and analyse the signal characteristics of various adnexal lesions and their ADC (apparent diffusion coefficient) values on DWI.

## Material and methods

A prospective analytical cohort study was carried out in the Department of Radiology of our institute over a period of 18 months on patients referred to MRI for characterization of adnexal lesions detected on ultrasound. All the cases referred for MRI scan regarding evaluation of adnexal lesions over a period of 18 months were included in the study. The study was approved by our Institutional Ethical Committee. Informed consent was obtained from all the patients included in this study. A total of 55 patients, constituting 67 lesions, were studied. The subjects encompassed all age groups. Cases with a prior history of surgical intervention or chemotherapy for ovarian tumours were excluded.

A 1.5 Tesla Magnetom Symphony Maestro class MRI (Siemens) was used to acquire the images. MR imaging protocol included Axial T1-weighted (TR/TE, 614/11 ms), T2W (TR/TE, 3350/98 ms) in axial, sagittal, and coronal planes, T1 Fat Saturation (T1 FS) in an axial plane. Diffusion-weighted images (TR/TE 4800/83 ms, slice thickness 4 mm, FOV 227-267 mm, matrix 102 × 160, and an acquisition time of 4 min) were acquired in the axial plane by using a single-shot echo-planar imaging sequence with b values of 0, 100, and 800. T1W FS images following IV gadolinium were acquired wherever necessary in axial, sagittal, and coronal planes.

## Image analysis

The lesions were evaluated and classified based on the site of origin, size, and signal characteristics in T1/T2/T1FS images on conventional MRI.

Analysis of DWI: Both qualitative (signal intensity) and quantitative-apparent diffusion coefficient (ADC) values of the lesions were recorded.

Qualitative analysis: The lesions were described as hypo-, iso-, hyperintense on DWI based on their signal intensities compared with the uterine myometrium.

Quantitative analysis: The apparent diffusion coefficient values were calculated on the workstation with standard software (Diffusion Calculation) using a circular operator-defined region-of-interest (ROI) measuring 3 mm, placed on the cystic/solid components or both (if the lesion had both solid and cystic). The ROI was placed away from the wall of the lesion and septations in cases of multiloculated lesions. In large lesions, the mean value of 3 different ROI measurements on the same slice was cal-

culated. In solid lesions, the necrotic core was avoided for calculations. In lesions showing components/locules with large differences in ADC values, both the highest and the lowest values were recorded. Analysis was done separately using the mean of lowest and of the highest values.

## Statistical analysis

Statistical analysis was done using SPSS windows software, version 20. Statistical significance of non-descriptive variables (ADC values of benign and malignant lesions) was calculated using the independent samples test – *t*-test. The ADC values of solid and cystic components were evaluated separately. The statistical analysis was done comparing the benign solid lesions with solid components of malignant lesions and cystic fluid of the benign lesions with cystic components of malignant lesions. Evaluation of descriptive variants such as signal intensity of the solid components on T2W and DW imaging was calculated using cross tabulation  $\chi^2$  test. In both the above analyses *p*-values < 0.05 were considered significant.

## Final confirmation

The diagnosis made on MRI was confirmed with the final clinical diagnosis made on the consensus of clinical setting/laboratory parameters/operative findings/follow-up. Guided biopsies were performed from the solid components of solid-cystic lesions (where feasible and accessible) of more than 10 cm in size with ascites. Solid lesions with a benign diagnosis on MRI were surgically excised. Lesions showing purely cystic components were followed up for a period of 6 months if the lesion size was less than 5 cm. Cystic lesions more than 5 cm were surgically excised.

## Results

Of the 55 patients studied, 12 (22%) had bilateral adnexal lesions resulting in 67 lesions. In cases with bilateral lesions, the morphology/histology of the lesions was similar in our study. The mean age of the patients in the study was 58 years, and 14 were postmenopausal.

Sixteen of the studied lesions were diagnosed as malignant, 50 as benign and 1 as borderline. For statistical purposes, the borderline tumour was included among the malignant lesions. The final diagnosis of various lesions encountered in our study is presented in Table 1. Table 2 depicts the lesion sizes encountered in our study.

The lesions were classified based on morphology as purely cystic, predominantly solid, and mixed solid and cystic.

## The pattern in solid components of lesions

Of the 16 malignant lesions, 5 (2 metastatic, 2 leiomyosarcoma, and 1 Sertoli-Leydig cell tumour) were pre-

**Table 1.** Final diagnosis of lesions

S. No.	Lesion	Number of lesions
1.	Primary ovarian malignancy	11: 6 – epithelial adenocarcinoma, 2 – transitional carcinoma, 2 – undifferentiated carcinomas, 1 – papillary carcinoma
2.	Metastasis	2 – LMS, 2 – others
3.	Sertoli-Leydig cell tumour	1
4.	Fibroids	6
5.	Fibrothecoma	2
6.	Haemorrhagic cysts	5
7.	Endometriomas	9
8.	Dermoid cysts	3
9.	Cystadenoma	3 – serous cystadenoma, 2 – mucinous cystadenoma
10.	Simple cysts	18
11.	Abscesses	2
12.	Borderline tumour	1

dominantly solid in composition, with mixed solid and cystic components in 11. The solid components of all the malignant lesions were hyperintense on T2W images and DWI except the Sertoli-Leydig tumour, which showed isointense signal. Eight of the benign lesions were solid in composition. Three of the 8 benign lesions

**Table 2.** Distribution of lesion sizes

S. No.	Diagnosis	Range of size, cm (largest dimension)
1.	Malignant ovarian lesions	10-12
2.	Sertoli-Leydig cell tumour	3
3.	Benign cystic lesions – haemorrhagic/endometrioma/simple cyst	5-7
4.	Dermoid cysts	7
5.	Abscess	10
6.	Fibrothecoma	12
7.	Fibroids	4-5
8.	Degenerated fibroids	7

(2 fibrothecoma and 1 fibroid with myxoid degeneration) showed hyperintense signal on T2W and DWI images with the remaining 5 showing hypointense signal.

Hyperintense signal of the solid component on T2W and DW images was significantly associated with malignancy and hypointense signal with benignity ( $p = 0.003$  and  $p = 0.001$ , respectively).

The ADC values of the benign and malignant lesions are shown in Table 1.

Amongst the benign lesions ( $n = 9$ ), there were 6 leiomyomas/fibroids, 1 case of ovarian torsion, and 2 fibrothecomas. The case of torsion ovary was excluded from the statistical analysis. The leiomyomas showed hypoin-

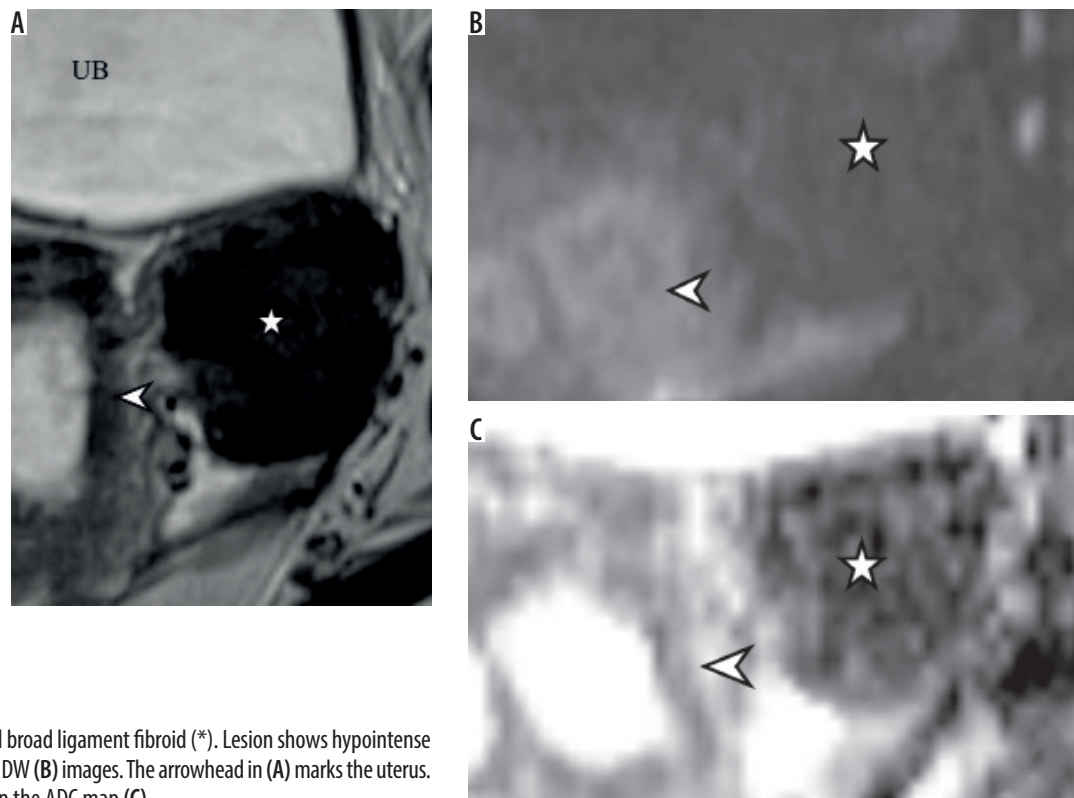


**Figure 1.** Left adnexal broad ligament fibroid (\*). Lesion shows hypointense signal on T2W (A) and DW (B) images. The arrowhead in (A) marks the uterus. Note the low signal on the ADC map (C)

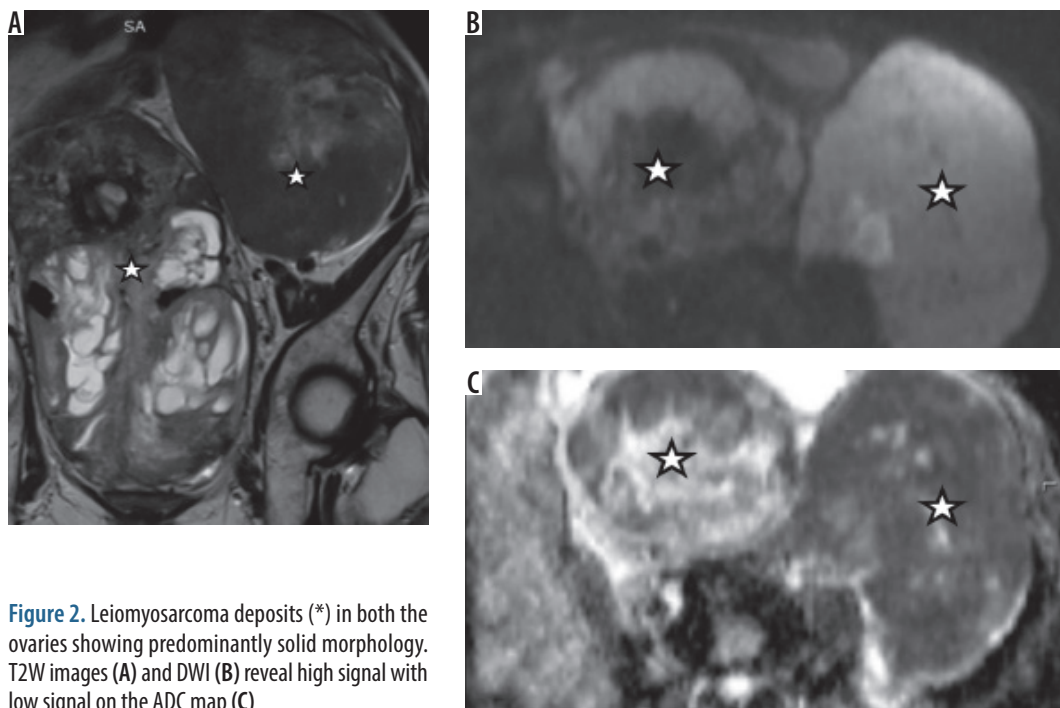


**Figure 2.** Leiomyosarcoma deposits (\*) in both the ovaries showing predominantly solid morphology. T2W images (A) and DWI (B) reveal high signal with low signal on the ADC map (C)

tense signal on T1/T2/DWI (Figure 1). Degenerated fibroids showed intervening patchy areas of high T2 signal with no restricted diffusion. A case of myxoid degeneration of fibroid showed a hyperintense signal on T2W and DWI with no loss of signal on ADC maps.

Leiomyosarcoma (LMS) deposits showed a hyperintense signal on T2W and DW imaging with restricted diffusion (Figure 2); ADC values were higher than leiomyoma (Table 1).

The mean ADC value of malignant lesions was  $0.87 \times 10^{-3} \text{ mm}^2/\text{s}$  (Table 2). Necrotic/cystic components did not show any diffusion restriction. The ADC value of leiomyomas without degeneration (mean:  $0.6 \times 10^{-3} \text{ mm}^2/\text{s}$ )

**Table 3.** Distribution of ADC values of solid components

Lesion	ADC values ( $\times 10^{-3} \text{ mm}^2/\text{s}$ )*	Mean
Leiomyoma	0.55	0.64
	0.63	
	0.76	
Degenerated leiomyoma	1.5	1.5
	1.5	
Fibroid with myxoid degeneration	1.7	
Fibrothecoma	0.6	0.75
	0.9	
Leiomyosarcoma	0.86	0.87
	0.89	
Sertoli-Leydig tumour	1.3	
Metastatic tumours	0.84	

\*The ADC vales of fibroids are lower than the malignant lesions and leiomyosarcoma.

was lower than the normal myometrium, as well as that of malignant lesions. However, fibroids showing degeneration showed a higher ADC value (mean:  $1.7 \times 10^{-3} \text{ mm}^2/\text{s}$ ) (Table 3).

Fibrothecoma showed a hyperintense signal on T2W and DW images (Figure 3), with a mean ADC value of  $0.75 \times 10^{-3} \text{ mm}^2/\text{s}$ . They were wrongly classified as malignant lesions (false positive).

When ROC curves were plotted with the ADC values of the solid components, a cut-off value of  $0.77 \times 10^{-3} \text{ mm}^2/\text{s}$  showed 93% sensitivity with a false positive rate of 5% for diagnosing benign lesions.

There was no statistical significance to the ADC values of the solid components for differentiating malignant from benign lesions (Table 4).

**Pattern in cystic lesions/cystic components of solid lesions**

Of the benign lesions, 42 were cystic in nature. The cystic fluid showed varying signal intensity on T1W images based on the fluid contents. Lesions containing blood products such as endometriomas, haemorrhagic cysts, and ruptured ectopic showed T1/T1FS hyperintense signal. The endometriotic cysts showed a drop in T2 signal (shading effect). Dermoid cysts showed T1 hyperintense signal with a drop in signal on T1FS. Other lesions showing a hyperintense signal on T1W images were abscesses and a few locules of mucinous cystadenoma. The borderline ovarian tumour showed predominantly cystic morphology with a few thick septations and small mural excrescences.

The diagnosis of a large convoluted hydrosalpinx was easier on MRI because of better anatomical delineation

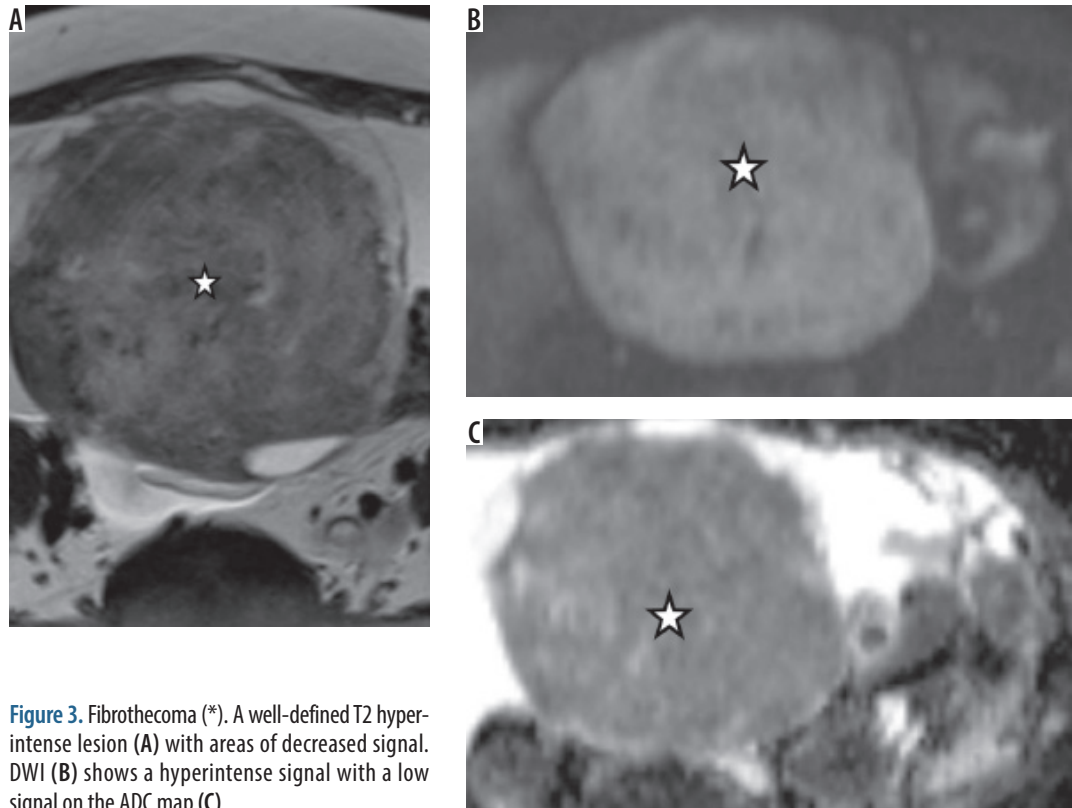


**Figure 3.** Fibrothecoma (\*). A well-defined T2 hyperintense lesion (A) with areas of decreased signal. DWI (B) shows a hyperintense signal with a low signal on the ADC map (C)

(visualization of ovaries separate from the lesion, retort-shaped lesions).

Two endometriotic cysts and an abscess showed fluid–fluid levels with one component showing a high signal on DWI. A corresponding decrease of signal in ADC maps s/o diffusion restriction was noted in abscesses (Figure 4).

**Table 4.** Mean ADC values of solid components of benign and malignant lesions

	Number (n)	Mean ADC	SD	p-value
Benign	8	0.87	0.17	0.290
Malignant	16	1.01	0.47	

\*  $\chi^2$  test shows no significant association between ADC value and lesion type.

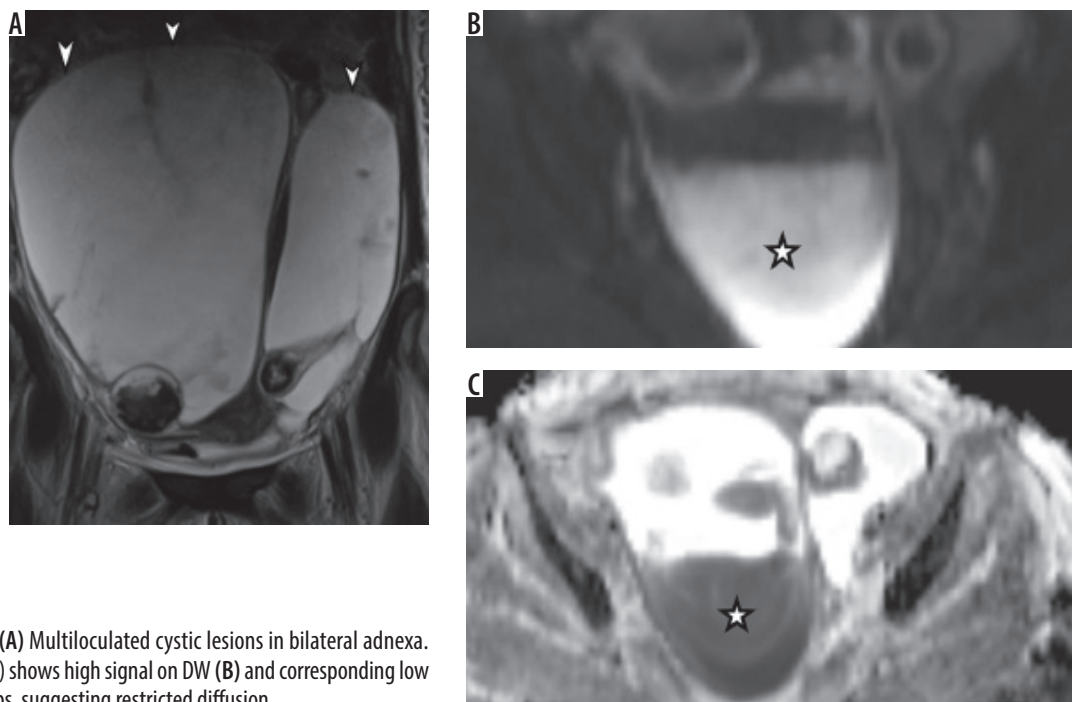


**Figure 4.** Abscesses: (A) Multiloculated cystic lesions in bilateral adnexa. Dependent portion (\*) shows high signal on DW (B) and corresponding low signal on ADC (C) maps, suggesting restricted diffusion

**Table 5.** Distribution of ADC values of the cystic fluid in benign and malignant lesions

Lesion	Mean ADC value ( $\times 10^{-3}$ mm <sup>2</sup> /s)	Standard deviation
Haemorrhagic and endometriotic cysts	1.2	0.16
Dermoid cysts	1.0	0.30
Simple cysts	2.3	0.43
Cystadenoma	2.65	0.20
Abscesses	1.4	0.89
Cystic components of malignant lesions	2.4	0.43

On DWI, dermoid cysts showed areas of hyperintense signal. ADC maps revealed low values in lipid components ( $0.5-0.7 \times 10^{-3}$  mm<sup>2</sup>/s).

Five benign cystic ovarian neoplasms, 3 serous, and 2 mucinous were encountered in our study. Both were thin-walled cystic lesions with no solid components/mural nodules. Serous cystadenomas were unilocular with T1 hypo- and T2 hyperintense signals. The mucinous lesions, on the other hand, were multiloculated and showed locules of varying signal intensity. The cysts did not show a low signal on ADC maps.

The ADC values of the cystic components of the lesions are shown in Table 3. The mean ADC value of benign cysts (all lesions included) was lower than the cystic components in malignant tumours (Table 5). When the ADC values of fluid in malignant lesions and benign cystic lesions (excluding cysts with haemorrhage and fat) were analysed there was no significant association of ADC with malignancy (Table 6).

ROC curves were plotted for the ADC values of the cystic lesions and cystic components of malignant lesions. A cut-off value of  $2.4 \times 10^{-3}$  mm<sup>2</sup> had a sensitivity of 88% with a false positive rate of 6% for diagnosing malignant lesions.

## Discussion

MRI has been used as a problem-solving tool in the diagnosis of adnexal lesions - in determining their site of origin and characterizing their tissue content [4,5]. Adnexal lesions may arise from the fallopian tubes, ovaries, or the uterus (pedunculated or broad ligament fibroids). Both benign and malignant ovarian lesions may show complex cystic/solid- cystic imaging morphology [6] resulting in a diagnostic dilemma. Many studies [7,8] found that the imaging features favouring malignancy in pre-operative scans were lesion size > 6 cm, thickness of the walls and septa > 3 mm, papillary projections, mural nodules, solid components, necrosis, haemorrhage, and intense enhancement of the solid components following administration of intravenous contrast.

The differentiation of benign from malignant lesions is pivotal for patient management in terms of surgical approach, the extent of surgical excision, and the need for post-surgical chemotherapy [9,10].

The signal of tissues on DWI is a function of their T2 characteristics and restricted water diffusion, and therefore diffusion-weighted images should be interpreted along with the ADC images. Highly cellular tissues such as malignancies restrict the movement of water molecules resulting in high signal intensity on DWI. This property has been used in the diagnosis of malignancies in gynaecological imaging [2,3,11,12].

Hyperintense signal of solid components on T2 and DWI was significantly associated with malignancy in our study, consistent with previous studies [13-15]. Hypointense signal in solid components reflecting the presence of fibrous stroma was similarly associated with benignity of the lesion [16].

Of the 30 benign and 47 malignant lesions studied by Thomassin Nagara *et al.* [13], low signal intensity on T2W and b1000 images were predictive of benignity with a positive likelihood ratio of 5.7 and 10.9, respectively. Similarly, a high b1000 signal with intermediate signal on T2W images was predictive of a malignant lesion with

**Table 6.** Mean ADC values of cystic components of benign and malignant lesions

Mean ADC values of all cystic fluid – benign and malignant				
	<i>n</i>	Mean	Std. deviation	
Benign	42	1.95	0.662	
Malignant	12	2.44	0.360	
Mean ADC values of cystic fluid – benign (excluding haemorrhagic and dermoid cysts) and malignant				
	<i>n</i>	Mean	Std. deviation	<i>p</i> -value
Benign	25	2.33	0.652	0.672
Malignant	12	2.44	0.360	

\* $\chi^2$  test shows no significant association between ADC value and lesion type when haemorrhagic and dermoid cysts are excluded.

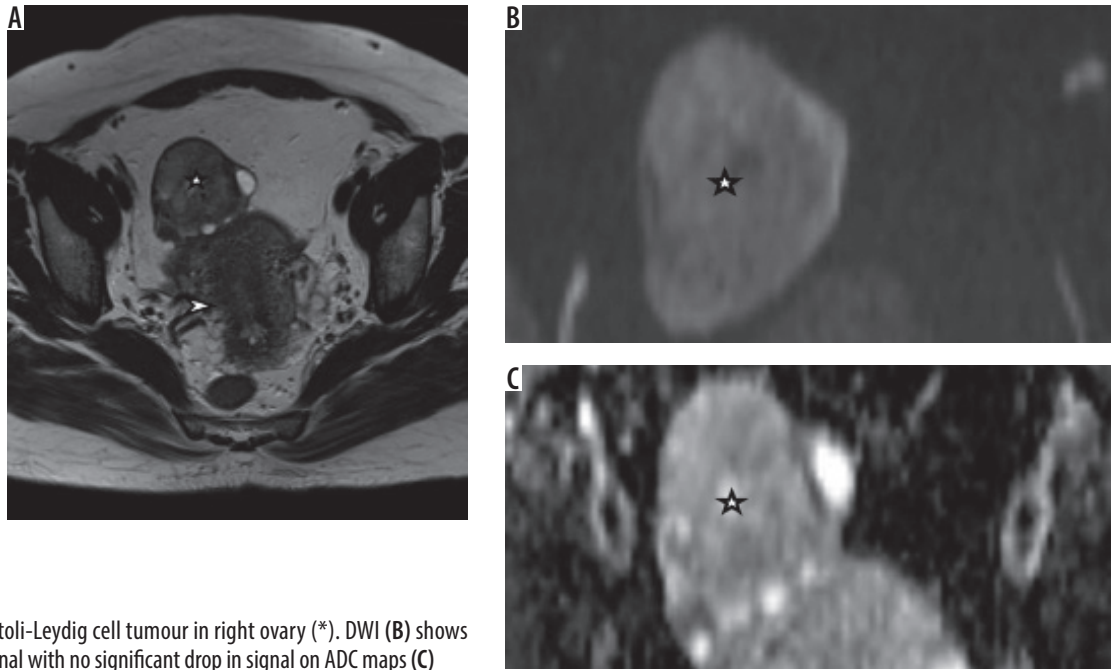


**Figure 5.** A) Sertoli-Leydig cell tumour in right ovary (\*). DWI (B) shows an isointense signal with no significant drop in signal on ADC maps (C)

a positive likelihood ratio of 4.5. In a study involving 202 solid and complex ovarian lesions, Zhang *et al.* [17] demonstrated that the presence of a high signal on T2W images and DWI with low ADC was predictive of malignancy. The presence of solid components with high signal on T2, DWI with high ADC values, or hypointense signal on T2/DWI and ADC maps was predictive of benignity. They had taken an ADC cut-off value of  $1.2 \times 10^{-3} \text{ mm}^2/\text{s}$ .

In our study, a cut-off value of  $0.7 \times 10^{-3} \text{ mm}^2/\text{s}$  yielded a sensitivity of 93% and a false positive rate of 5%. Based on the ROC there is no significance of ADC values in distinguishing benign from malignant lesions. This result is probably due to the number (8 benign vs. 16 malignant) and the histology (most benign lesions being fibroids, which show low ADC values) of the lesions.

Two benign lesions falsely classified as malignant in our study were fibrothecomas. High signal on DWI was found in the 3 highly cellular fibrothecomas in a study conducted by Takeuchi *et al.* [14]. All these lesions showed interspersed focal areas of T2 hypointense solid components [14]. Similar findings were noted in our study along with ascites. The hyperintense signal on T2/DWI in fibrothecomas is attributed to the presence of theca-like cells with lipid-rich content and stromal oedema [18]. The ADC values of fibrothecoma are reflective of its fibrous content; the more fibrous the tissue, the lower the values [19].

A case of malignant Sertoli-Leydig cell tumour presenting with symptoms of hirsutism was encountered in our study. The tumour showed a solid morphology, presence of microscopic fat on chemical shift imaging, heterogeneous moderate enhancement on contrast images, an isointense signal on DWI, and ADC values higher than the rest of the malignant lesions (Figure 5). The lesion

could be correctly classified on conventional imaging as malignant but not on DWI alone.

Leiomyomas with no changes of degeneration in our study had low signal on T2W/DWI and low ADC values similar to previous studies [13,17]. Degenerated fibroids had ADC values higher than the non-degenerated fibroids. Fibroids with degenerative changes and myxoid degeneration showed high signal in ADC maps corresponding to the regions with high T2/DWI signal due to the T2 “shine through” effect [20,21].

Leiomyosarcoma (LMS) deposits, in contrast to leiomyoma (fibroids), showed hyperintense signal intensity on T2W and DW images with low ADC values ( $0.8 \times 10^{-3} \text{ mm}^2/\text{s}$ ). DWI can thus help differentiate leiomyosarcomas from degenerated fibroids when evaluated in conjunction with signals on ADC maps.

High signal on T2W and DWI was considered diagnostic of sarcomatous change in pre-existing fibroids in addition to hyperintense signal on T1W images suggesting haemorrhage [22]. However, later studies concluded that T1/T2/DW hyperintense signals in a fibrous lesion are not diagnostic but should raise suspicion for sarcomatous change [23].

The low ADC values seen in fibroids can be attributed to “the black-out effect” resulting from the presence of fibroblasts producing a dense collagen matrix [21]. Hence, ADC values do not contribute to the differentiation of benign from malignant solid lesions when considered in isolation [13,19].

The role of DWI in diagnosing cystic lesions of the adnexa is limited because of diffusion restriction demonstrated by many benign lesions [21]. Haemorrhagic cysts, endometriomas, dermoid cysts, mucinous cystic tumours,

and abscesses can all show areas of diffusion restriction with low ADC values.

Cystic teratomas show a characteristic high signal intensity on T1W images, which is suppressed on T1W FS images and can be diagnosed accurately on conventional MRI [24]. Keratinous or epidermoid components within these cysts may show diffusion restriction [21,25].

Lesions containing blood products such as haemorrhagic and endometriotic cysts show high signals on T1W/T1W FS images. The endometriotic cysts show a characteristic drop in signal on T2W images known as the “shading effect” [26] due to the presence of hemosiderin and proteinaceous contents [27,28]. It is for the same reason that infective lesions such as abscesses can present as complex lesions with varying intensities on T1W and T2W images. Abscesses show diffusion restriction due to internal viscous contents (pus) and cell debris [29,30]. However, the clinical history and signal characteristics on conventional imaging aid in the diagnosis.

The cystic components of malignant lesions do not show diffusion restriction. With a cut-off of  $2.2 \times 10^{-3}$  mm<sup>2</sup>/s, differentiation of benign from malignant lesions showed a false positive rate of 6.4%. Therefore, based on the ADC values of the cystic components, we cannot differentiate benign from malignant adnexal masses. When ADC values of all benign cystic lesions (excluding haemorrhagic and dermoid cysts) and cystic components of

malignant lesions were compared, the mean ADC value of the benign lesions ( $2.3 \times 10^{-3}$  mm<sup>2</sup>/s) was lower than that of malignant lesions ( $2.5 \times 10^{-3}$  mm<sup>2</sup>/s). The increased ADC value in cystic components of malignant lesions has been attributed to turbulent flow in large lesions due to the compressions by respiratory efforts known as “the sloshing effect” [31].

### Limitations of the study

The number of benign lesions exceeded the number of malignant lesions.

### Conclusions

Qualitative DWI acts as an adjunct to conventional MRI in differentiating benign from malignant adnexal lesions showing solid/mixed morphology. It plays no role in differentiating cystic lesions due to a significant overlap of lesion characteristics. Quantitative DWI/ADC values play no role in differentiating benign from malignant adnexal lesions, irrespective of lesion morphology. DWI should always be interpreted in conjunction with conventional MRI.

### Conflicts of interest

The authors report no conflict of interest.

### References

1. Timmerman D, Ameye L, Fischerova D, et al. Simple ultrasound rules to distinguish between benign and malignant adnexal masses before surgery: Prospective validation by IOTA group. *BMJ* 2010; 341: c6839. doi: 10.1136/bmj.c6839.
2. Kilickesmez O, Bayramoglu S, Inci E, et al. Quantitative diffusion-weighted magnetic resonance imaging of normal and diseased uterine zones. *Acta Radiol* 2009; 50: 340-347.
3. Namimoto T, Awai K, Nakaura T, et al. Role of diffusion-weighted imaging in the diagnosis of gynecological diseases. *Eur Radiol* 2009; 19: 745-760.
4. Spencer JA, Forstner R, Cunha TM, et al. ESUR guidelines for MR imaging of the sonographically indeterminate adnexal mass: an algorithmic approach. *Eur Radiol* 2010; 20: 25-35.
5. Thomassin-Naggara I, Aubert E, Rockall A, Jalaguier-Coudray A. Adnexal masses: development and preliminary validation of an MR imaging scoring system. *Radiology* 2013; 267: 432-443.
6. Forstner R, Meissnitzer T, Meissnitzer M. Benign lesions that mimic cancer: ovarian. *Cancer Imaging* 2015; 15 (Suppl 1): O22. doi: 10.1186/1470-7330-15-S1-O22.
7. Sohaib SA, Sahdev A, Van Trappen PO, et al. Characterization of adnexal mass lesions on MR imaging. *AJR Am J Roentgenol* 2003; 180: 1297-1304.
8. Hricak H, Chen M, Coakley FV, et al. Complex adnexal masses: detection and characterization with MR imaging – multivariate analysis. *Radiology* 2000; 214: 39-46.
9. Abdelsalam SM, Hamed ST, Sayed MA. Diagnostic performance of GI-RADS reporting system in evaluation of adnexal masses. *Egypt J Radiol Nucl Med* 2020; 51: 60. doi: <https://doi.org/10.1186/s43055-020-00155-9>.
10. Watanabe E, Tanaka K, Takeda N, et al. Surgical technique to prevent spillage of cyst fluid during operation for cystic ovarian tumors. *Pediatr Surg Int* 2013; 29: 645-649.
11. Whittaker CS, Coady A, Culver L, et al. Diffusion-weighted MR imaging of female pelvic tumors: a pictorial review. *Radiographics* 2009; 29: 759-774.
12. Koh DM, Collins DJ. Diffusion-weighted MRI in the body: applications and challenges in oncology. *AJR Am J Roentgenol* 2007; 188: 1622-1635.
13. Thomassin-Naggara I, Darai E, Cuenod CA, et al. Contribution of diffusion weighted MR imaging for predicting benignity of complex adnexal masses. *Eur Radiol* 2009; 19: 1544-1552.
14. Takeuchi M, Matsuzaki K, Nishitani H. Diffusion weighted magnetic resonance imaging of ovarian tumors: differentiation of benign and malignant solid components of ovarian masses. *J Comput Assist Tomogr* 2010; 34: 173-176.
15. Koyama T, Togashi K. Functional MR imaging of the female pelvis. *J Magn Reson Imaging* 2007; 25: 1101-1112.
16. Cappabianca S, Iaselli F, Reginelli A, et al. Value of diffusion-weighted magnetic resonance imaging in the characterization of complex adnexal masses. *Tumori Journal* 2013; 99: 210-217.

17. Zhang P, Cui Y, Li W, et al. Diagnostic accuracy of diffusion-weighted imaging with conventional MR imaging for differentiating complex solid and cystic ovarian tumors at 1.5T. *World J Surg Oncol* 2012; 10: 237. doi: 10.1186/1477-7819-10-237.
18. Yin B, Li W, Cui Y, et al. Value of diffusion-weighted imaging combined with conventional magnetic resonance imaging in the diagnosis of thecomas/fibrothecomas and their differential diagnosis with malignant pelvic solid tumors. *World J Surg Oncol* 2016; 14: 5. doi: 10.1186/s12957-015-0760.
19. Agostinho L, Horta M, Salvador JC, Cunha TM. Benign ovarian lesions with restricted diffusion. *Radiol Bras* 2019; 52: 106-111.
20. Morisawa N, Kido A, Koyama T, et al. Changes of the normal ovary during menstrual cycle in reproductive age on the diffusion-weighted image. *J Comput Assis Tomogr* 2012; 36: 319-322.
21. Duarte AL, Dias JL, Cunha TM. Pitfalls of diffusion-weighted imaging of the female pelvis. *Radiol Bras* 2018; 51: 37-44.
22. Gaetke-Udager K, McLean K, Sciallis AP, et al. Diagnostic accuracy of ultrasound, contrast-enhanced CT, and conventional MRI for differentiating leiomyoma from leiomyosarcoma. *Acad Radiol* 2016; 23: 1290-1297. doi: 10.1016/j.acra.2016.06.004
23. Suzuki A, Aoki M, Miyagawa C, et al. Differential diagnosis of uterine leiomyoma and uterine sarcoma using magnetic resonance images: a literature review. *Healthcare (Basel)* 2019; 7: 158.
24. Outwater EK, Siegelman ES, Hunt JL. Ovarian teratomas: tumor types and imaging characteristics. *Radiographics* 2001; 21: 475-490.
25. Namimoto T, Awai K, Nakaura T, et al. Role of diffusion-weighted imaging in the diagnosis of gynecological diseases. *Eur Radiol* 2009; 19: 745-760.
26. Siegelman ES, Oliver ER. MR imaging of endometriosis: ten imaging pearls. *RadioGraphics* 2012; 32: 1675-1691.
27. Mansour S, Wessam R, Raafat M. Diffusion-weighted magnetic resonance imaging in the assessment of ovarian masses with suspicious features: strengths and challenges. *Egypt J Radiol Nucl Med* 2015; 46: 1279-1289.
28. Corwin MT, Gerscovich EO, Lamba R, et al. Differentiation of ovarian endometriomas from hemorrhagic cysts at MR imaging: utility of the T2 dark spot sign. *Radiology* 2014; 271: 126-132.
29. Takeshita T, Ninoi T, Doh K, et al. Diffusion-weighted magnetic resonance imaging in tubo-ovarian abscess: a case report. *Osaka City Med J* 2009; 55: 109-114.
30. Li W, Zhang Y, Cui Y, et al. Pelvic inflammatory disease: evaluation of diagnostic accuracy with conventional MR with added diffusion-weighted imaging. *Abdom Imaging* 2013; 38: 193-200.
31. Kim HJ, Lee SY, Shin YR, et al. The value of diffusion-weighted imaging in the differential diagnosis of ovarian lesions: a meta-analysis. *PLoS One* 2016; 11: e0149465. doi: 10.1371/journal.pone.0149465.